Enabling the Direct Detection of Earth-sized Exoplanets with the LBTI HOSTS Project: A Progress Report

W. Danchi[1a], V. Bailey[b], G. Bryden[c], D. Defrère[b], S. Ertel[b], C. Haniff[d], P. Hinz[b], G. Kennedy[d], B. Mennesson[c], R. Millan-Gabet[e], G. Rieke[b], A. Roberge[a], E. Serabyn[c], A. Skemer[b], K. Stapelfeldt[a], A. Weinberger[f], M. Wyatt[d], A. Vaz[b]

[a]NASA Goddard Space Flight Center, Greenbelt, MD; [b]University of Arizona, Tucson, AZ, [c]Jet Propulsion Laboratory, Pasadena, CA; [d]University of Cambridge, Cambridge, UK; [e] California Institute of Technology, Pasadena, CA; [f]Carnegie Institution, Washington, DC

ABSTRACT

NASA has funded a project called the Hunt for Observable Signatures of Terrestrial Systems (HOSTS) to survey nearby solar type stars to determine the amount of warm zodiacal dust in their habitable zones. The goal is not only to determine the luminosity distribution function but also to know which individual stars have the least amount of zodiacal dust. It is important to have this information for future missions that directly image exoplanets as this dust is the main source of astrophysical noise for them. The HOSTS project utilizes the Large Binocular Telescope Interferometer (LBTI), which consists of two 8.4-m apertures separated by a 14.4-m baseline on Mt. Graham, Arizona. The LBTI operates in a nulling mode in the mid-infrared spectral window (8-13 μm), in which light from the two telescopes is coherently combined with a 180 degree phase shift between them, producing a dark fringe at the location of the target star. In doing so the starlight is greatly reduced, increasing the contrast, analogous to a coronagraph operating at shorter wavelengths. The LBTI is a unique instrument, having only three warm reflections before the starlight reaches cold mirrors, giving it the best photometric sensitivity of any interferometer operating in the mid-infrared. It also has a superb Adaptive Optics (AO) system giving it Strehl ratios greater than 98% at 10 μm. In 2014 into early 2015 LBTI was undergoing commissioning. The HOSTS project team passed its Operational Readiness Review (ORR) in April 2015. The team recently published papers on the target sample, modeling of the nulled disk images, and initial results such as the detection of warm dust around η Corvi. Recently a paper was published on the data pipeline and on-sky performance. An additional paper is in preparation on β Leo. We will discuss the scientific and programmatic context for the LBTI project, and we will report recent progress, new results, and plans for the science verification phase that started in February 2016, and for the survey.

Keywords: debris disks, exozodiacal dust, stellar interferometry, nulling interferometry, exoplanet detection, infrared astronomy

1. INTRODUCTION

NASA is currently embarked on a long-term mission to search for exoplanets in the habitable zones of nearby sun-like stars, with the goal of detecting and characterizing rocky Earth-sized planets, which might have liquid water on their surfaces and oxygen in their atmospheres indicative of non-equilibrium atmospheric chemistry caused by life on those exoplanets.

Over the past two decades mission concepts have been developed at infrared and at visible wavelengths, initially called the Terrestrial Planet Finder – Interferometer (TPF-I) and the Terrestrial Planet Finder – Coronagraph (TPF-C), respectively [1]. The latter mission concept has provided the scientific and technical foundation for current studies of the Wide Field Infrared Space Telescope (WFIRST) - Astrophysics Focused Telescope Asset (AFTA) internal coronagraph, which utilizes one of two 2.4-m visible wavelength space telescopes donated by the intelligence community to NASA. Also last year NASA completed studies of two Probe-class mission concepts (~$1B USD), one

[1] william.c.danchi@nasa.gov; phone 1 301 286-4586; fax 1 301 286-7230

Optical and Infrared Interferometry and Imaging V, edited by Fabien Malbet, Michelle J. Creech-Eakman, Peter G. Tuthill, Proc. of SPIE Vol. 9907, 990713
 · doi: 10.1117/12.2233397

with an internal coronagraph on a 1+ m class telescope, called Exo-C [2], a concept called Exo-S, with a telescope of a similar size and a moderately-sized starshade [3]. These activities stem from the endorsement by Astro2010 Decadal Survey [4] of the search for new worlds. The survey chose the WFIRST mission as its top priority for large missions, and the New Worlds Technology Development Program, was selected to be the top priority in the medium-size mission category. The probe-class mission concepts were studied in case the WFIRST-AFTA - coronagraph mission was not brought into the implementation phase. However, during this past fiscal year, WFIRST-AFTA with a coronagraph baselined for the mission passed extensive reviews and entered into a Phase A start.

The search for life on planets around other worlds is observationally extremely difficult for two main reasons. First, at visible wavelengths (at around 600 nm) the contrast-ratio between the star and the reflected light for the planet when the planet is at maximum elongation is of the order of 10^{-10} and the contrast ratio in the mid-infrared (10 μm) is of the order of 10^{-7}. Second, dusty disks, which are the remnants of the primordial protoplanetary disks in which the planets formed, act as a source of astrophysical background noise and source confusion in the measurements if the dust density is larger than about ten times that of our solar system and/or if the dusty material is clumpy, respectively [5].

Around our solar system, such dust is created by collisions of asteroids and the evaporation of comets. This warm dust extends from the asteroid belt inward to the point at which dust is sublimated by the heat from the Sun. Cold dust also exists in our solar system in the Edgeworth-Kuiper belt. The dust that affects observations of exoplanets in the habitable zone is the warm component of the dust, called exozodiacal dust by analogy with our own zodiacal dust.

The Astro2010 survey committee discussed the importance of determining exozodiacal dust levels around nearby stars and it specifically mentioned the *"... need to characterize the level of zodiacal light present so as to determine, in a statistical sense if not for individual prime targets, at what level starlight scattered from dust will hamper planet detection"* [4].

The effect of the exozodiacal dust on the performance of planet detection and characterization missions has been discussed in a paper by Roberge et al. [5]. These researchers showed that the integration time to detect a planet as a function of zodiacal dust levels (or zodi level) for coronagraphic instruments on telescopes of different diameters – 2- , 4-, and 8-meters. They showed that the integration time goes as the telescope diameter, D^{-4}, and linearly with the zodi level. Here we use the term "zodi" to mean that the detected emission is equivalent to that of our own solar system, using the optical depth and vertical and in plane density and temperature structure of the debris disk as defined by the Kelsall model (Kelsall et al. [6]).

Recently, Defrère et al. [7] examined the detectability of exo-Earths in clumpy debris disks, using a collisional grooming algorithm that simultaneously solves the equations of motions of small dust grains, including interactions with a planet on a circular orbit around the host star, and number flux equations that includes the destruction of grains via grain-grain collisions, as discussed in detail in the paper by Stark et al. [8]. The results of the model employed by Defrère et al. [7] are shown in Figure 1. Here the effect of exozodi on the detectability of the Sun-Earth system at 10 pc is displayed in a series of images that are produced by a PIAA coronagraph, and an exozodi cloud corresponding to 1, 5, and 10 times the solar system zodi level (left two columns), and 20, 50, and 100 zodis on the right two columns. The images on the left of each set of two columns are the images from the PIAA coronagraph itself, and on the right the result of a PSF fitting algorithm that fits and subtracts the zodi from the images. Note that starting on the bottom left corner at a level of approximately 10 zodis, an additional detection is made a few degrees from the location of the Earth, which is from a dust clump, created by planet trailing grains that were included in the model (Stark et al. [8]). At zodi levels of 20 or higher the Earth itself becomes increasing difficult to detect, and the algorithm instead consistently finds only the dust clump.

This paper describes progress on a ground-based survey designed to measure the mean level of exozodiacal dust (exozodi) in the habitable zone around nearby solar type stars and the level of exozodi around nearby important target stars for direct imaging missions. This survey, funded by NASA, utilizes the unique Large Binocular Telescope Interferometer (LBTI). Formally it is called the Hunt for Observable Signatures of Terrestrial Planets (HOSTS) program. The overall HOSTS teams includes an LBTI instrument team led by Principal Investigator, P. Hinz, instrument scientists D. Defrère and S. Ertel, and a science team competitively selected by NASA. This paper is one of several contributions by the team for this conference. An overview of the LBTI as an interferometer and general purpose L, M, and N band imager by Hinz et al. [9] [9907-03] was presented on Monday. Defrère et al. [10] (9907-50) presented a paper on improvements to the system that are in progress. The nulling precision of the LBTI is being improved by measuring and correcting the differential path length between the two telescopes, caused by fluctuations in the

Precipitable Water Vapor (PWV) of their atmospheric columns. Improvements to the precision of the null depth and associated parameters, based on the statistical behavior of the null data utilize an analysis technique called Null Self-Calibration (NSC), are presented in a paper by Mennesson et al. [11] (9907-32)

For the remainder of this paper we discuss progress on the exozodiacal dust problem, emphasizing the growing body of results for debris disk architectures that vary between different stars included cold, hot, and warm dust. Interesting correlations are just beginning to emerge. Next, we briefly discuss the LBTI instrument, and some recent papers from the HOSTS team, including ones on the HOSTS sample, modeling, first results, and on data reduction and on-sky performance, and the status and future of the project.

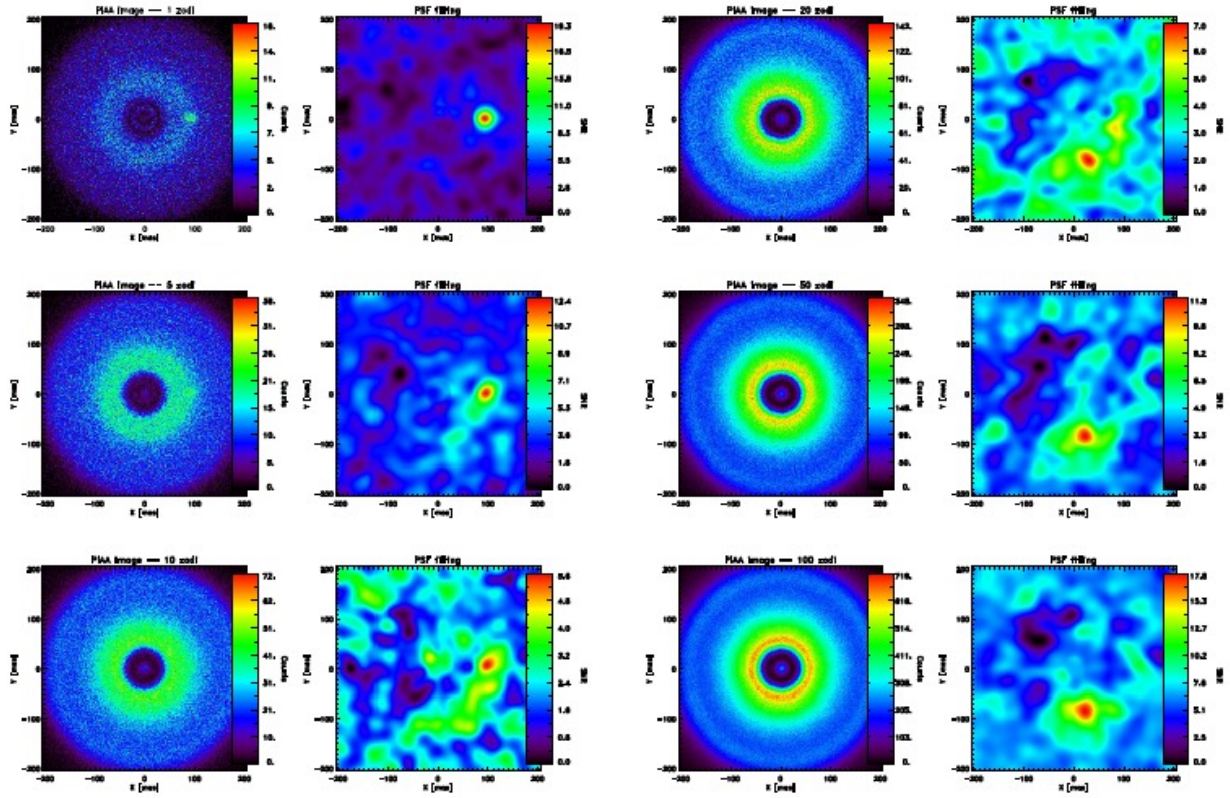

Figure 1. Images from the paper by Defrère et al. [7] displaying the effect of exozodi on the detectability of the Sun-Earth system at 10 pc, in which the images are produced by a PIAA coronagraph, and an exozodi cloud corresponding to 1, 5, and 10 times the solar system zodi level on the left column, and 20, 50, and 100 zodis on the right column. The images on the left of each column are the images from the PIAA coronagraph itself, and on the right the result of a PSF fitting algorithm that fits and subtracts the zodi from the images. Note that starting on the bottom left corner at a level of approximately 10 zodis, an additional detection is made a few degrees from the location of the Earth, which is from a dust clump, created by planet trailing grains that were included in the model [7]. At zodi levels of 20 or higher the Earth itself becomes increasing difficult to detect, and the algorithm instead consistently finds only the dust clump.

2. THE STATE OF EXOZODIAL DUST OBSERVATIONS

2.1 Cold Dust

Observationally studies of the exozodi began with discoveries from a succession of cooled infrared satellites -- *IRAS, ISO, Spitzer* and *Herschel* -- that allowed astronomers to search for infrared excesses in the Spectral Energy Distributions (SEDs) of main-sequence stars in the solar neighborhood.

For this paper we focus primarily on F, G, and K spectral types of nearby stars that are most important from a exoplanet detection standpoint. However, we begin briefly with some important results that firmly established the nature and

existence of exozodiacal dust as debris material remaining after the protoplanetary disk was dissipated following the formation of exoplanets.

Using the 24 μm channel of the MIPS photometer on *Spitzer*, Rieke et al. [12], [13] performed a study of 266 main-sequence A stars within a distance of 150 pc of the Sun. They showed that the fraction of stars with an excess (as compared to that of the emission from the photosphere) decreased from ~25% for the youngest stars in the sample (~10 Myr) to ~1% for stars older than >190 Myr. Strong excesses were observed well past the initial falloff (~500 Myr) indicating that dust was being created in episodic collisions of asteroids or other small bodies within these systems.

Focusing on nearby F, G, K stars observed by Spitzer, Bryden et al. [14] found that 14 of 146 stars in their sample had infrared excesses at 24 and/or 70 μm, with just a single star with an excess only at 24 μm. The remaining 13 stars had stronger emission at 70 μm consistent with cold dust >10 AU from the star. These authors found a marginally lower detection rate for stars with planets than those without planets, but the result was inconclusive as the observed difference was not statistically significant. Lawler et al. [15] used data from the 30-34 μm band of the IRS instrument on Spitzer, with a sample of 152 nearby stars. They found the fraction of stars with an excess was about 12%, similar to that of Bryden et al. [16]. However, the fraction at the short wavelength band (8.5-12 μm) was only 1%. These observations constrained the mean zodiacal dust level to be less than 1000 times that of the solar system for warm dust, and 100 times that of the solar system for cool dust. No correlation was seen with metallicity or spectral type (Bryden et al. [14]), but all of the studies were consistent with an age correlation, i.e., stars less than 1 Gyr old were more likely to have excesses than older stars like the Sun.

Importantly, the observational limitations of debris disk surveys at 24 μm with *Spitzer* became evident as detections required fluxes more than 10% above the photosphere due to errors in estimation of the photospheric levels, as well as flat fielding errors (see Siercho et al. [17]; Bryden et al. [16]). At 70 μm the Spitzer observations were limited by extragalactic background source confusion and by Galactic cirrus (Bryden et al. [16]).

The *Herschel* Space Observatory had sufficient sensitivity (with the PACS instrument at 100 and 160 μm) to detect the emission from the equivalent of our own Edgeworth-Kuiper belt around nearby solar type stars. Two Open Time Key Projects were devoted to debris disk observations. The DUNES project (C. Eiroa, PI) focused on a volume-limited sample of 123 FGK stars within 25 pc of the Sun. The key feature of DUNES was that for each star the integration time is adjusted to detect its photosphere with SNR=5. The DEBRIS project (P.I., B. Mathews) observed a larger number of stars with the integration time adjusted to a particular flux density limit. Both projects shared 106 stars. The DUNES project increased the incidence rate of discs around the DUNES sample from ~12.1% +/- 5% before Herschel to 20.2% +/- 2%, and ~52% of detected disks were resolved (Eiroa et al. [18]).

Recently, Montesinos et al. [19] published a paper discussing the combined full sample of 177 stars from the DUNES survey, including 54 additional stars that were shared with the DEBRIS consortium, as well as the original partial sample of 123 stars published by Eiroa et al. [18]. Focusing on a subsample of 105 stars within 15 pc, Montesinos et al. [19] found incidence rates for different spectral types as follows, for F stars, the rate was 26% + 21% - 14% (6/23 F stars), for G stars 21% +17% - 11% (7/33 G stars), and K stars 20% + 14% -9% (10/49 K stars). Combining results from the all the spectral types taken together, the occurrence rate was 22% + 8% -7% (95% confidence level). They also found that the median zodi level, in terms of the ratio L_{dust}/L_{star} for each spectral type was 7.8×10^{-7} for F stars, 1.4×10^{-6} for G stars, and 2.2×10^{-6} for K stars. Another important finding from this work was that the incidence of debris disks was not particularly dependent on stellar age as indicated by the subsample of young active stars compared to the subsample of inactive older stars. However, as expected from collisional models, the fractional luminosity tended to decrease with increasing age, indicating a gradual erosion of the debris disks.

2.2 Hot Dust

Hot exozodi dust was detected several years ago using precision visibility measurements obtained with the FLUOR instrument on the CHARA array (di Folco et al. [20], Absil et al. [21], Absil et al. [22]) based on a sample of 42 stars with spectral types ranging from A to K stars over the time period from 2005 to 2011. The FLUOR instrument was able to obtain measurements of the squared visibility (V^2) with a precision of approximately 0.3% for the short baseline (S1 to S2) of CHARA of about 34 m. These measurements relied on observations of a small difference in V due to extended emission from hot exozodiacal dust at angular separations of 30 to 100 mas around nearby main sequence stars (Absil et al. [22]). The extended emission produced a small drop in V^2 compared to that expected from the stellar photosphere. During the survey one of the stars was eliminated, which was found to have a close companion. Of the remaining stars,

22 were known to have cold dust, and 19 were not known to have any dust. There were 12 A stars, 14 F stars, and 15 G or K stars. Of the final sample of 41 stars, 14 were found to have hot dust, but two detections were not considered significant, leaving the 12 with a K-band circumstellar excess, giving an incidence rate of 29% +8% -6% (> 3 sigma detections). The results on the survey of K-band excesses can be compared with those from the far-infrared surveys of cold dust from Spitzer and Herschel, and the survey of warm dust in the habitable zone, carried out by the Keck Interferometer a few years ago.

2.3 Warm Dust in the Habitable zone and Nulling Interferometry

There has been relatively little observational work on the warm component of debris disks, corresponding to dust in the habitable zone. Nulling interferometry has become the main technique used to observe this component of debris disks. With nulling interferometry an achromatic π phase shift is introduced between the electric fields coming from two telescopes before they are interfered, producing a broad-band dark fringe at the location of the host star, and bright fringes $\lambda/(2B)$ from the dark fringe where the interferometer is most sensitive to thermal emission from dust or a planet, where λ is the wavelength of observation and B is the interferometer baseline. This technique was invented by Bracewell [23] in the 1970's, however, it took many years before it was put into observational use. Infrared nulling instruments measure a quantity called the leakage, which is zero only for a perfect instrument with a point-like star. There is a minimum leakage due to instrumental errors such as residual wavefront and path-length errors, as well as the finite size of the host star. The leakage is the difference between the null signal from a target star minus the null signal from a reference star. The leakage can also be related to traditional interferometric quantities such as the visibility, where the null quantity, *N*, is given by $N = (1-V)/(1+V)$, where *V* is the magnitude of the complex visibility which is the Fourier transform of the brightness distribution of the source (see papers by Barry et al. [24], Serabyn et al. [25] for more detailed discussions).

Two studies focused on determining the mean level around nearby main-sequence stars. The first was published by Liu et al. [26] who used the BLINC-MIRAC instrument on the MMT, which had its AO system, the MMTAO, installed at that time. This study focused on six nearby stars: four A stars, one F, and one K star. No warm dust emission was detected from any of the objects, and the 3-σ upper limits ranged from 220 to 10,000 zodis. The second study was the Keck Interferometer Nuller (KIN) survey of 25 stars at N band (Millan-Gabet et al. [27]). There were 3 detections (η Crv, γ Oph, and α Aql), and 22 non-detections. The non-detections were consistent with a 3-σ mean zodi level less than 150 zodis, if all the stars were considered to be a single class of objects. For the KIN observations, the largest source of error was not the formal error due to the scatter in the calibrated leakages, but instead it was the night-to-night variation of the calibrated data on the same stars, which was called the "external" error (Millan-Gabet et al. [27], and Colavita et al. [28], [29]).

2.4 Recent Results on Warm Exozodi Dust Emission and Comparisons with Other Surveys

Recently, Mennesson et al. [30] published results from the complete KIN survey, with a total of 47 nearby main-sequence stars, including those from the originally published partial survey of 25 stars discussed previously. Measurements were presented from the 10 spectral channels from 8 to 13 μm as well as the highest signal-to-noise measurements from the 8-9 μm channel. This larger survey included 5 detections of excesses with significance greater 3σ (η Crv, β leo, β Uma, ζ Lep, and γ Oph) as well as 3 additional stars with probable excess, of significance 1-3σ, for a total of 8 detections out of a sample of 47 stars, or about a 17% detection rate. These additional stars were Fomalhaut, Vega, and Altair.

Figure 2 shows the statistical analysis of 40 stars that were considered "effectively single" in the paper. The left panel displays the histogram of excesses in the 8-9 μm band, showing that it is skewed towards stars displaying positive excesses, with five stars having significance above 3σ. The middle panel shows the same data, but now expressed in zodi units, showing a substantial number of the sample stars having excesses in the range of 150-450 zodis. Note also, the third panel, which includes the entire 8-13 μm band also shows a histogram skewed towards positive zodi excess with about 8 stars having excesses above 2σ.

Mennesson et al. [30] also explored correlations with the observations described in Sections 2.1 and 2.2 above, as seen in Figure 3. Here we see that excess rates observed in the mid-infrared by the Keck Nuller are compared with those known to have either far-infrared (cold), or near-infrared (hot) excesses, or none previously observed. For the Keck Nuller data in the 8-9 μm band, the mid-infrared (MIR) excess rate is defined as requiring and excess with significance

greater than 3σ. For the observations from 8 to 9 μm, only a significance of 2σ is used in the figure. Note that there is a strong correlation between detections of cold excesses at far-infrared (FIR) wavelengths, e.g., from Herschel or Spitzer SED observations at 70 μm or longer wavelengths. Interestingly for the most sensitive measurements with the Keck Nuller in the 8-9 μm band, there is essentially no correlation with the existence of hot dust detected in the near-infrared.

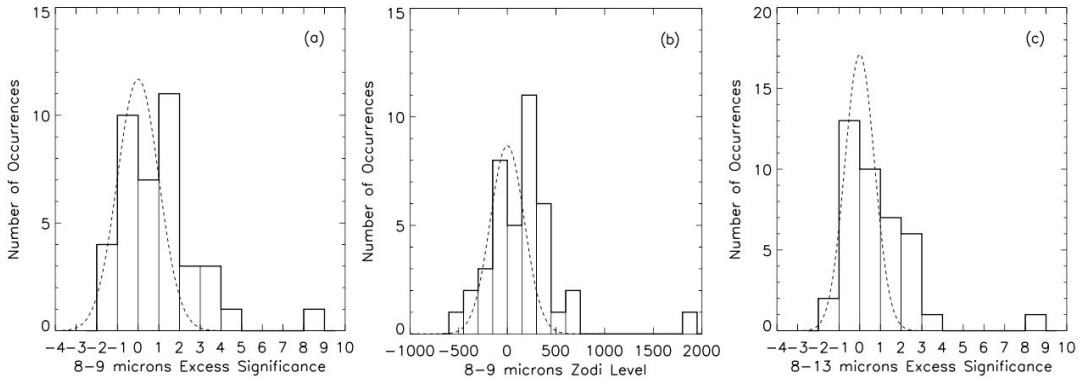

Figure 2. The left panel displays the histogram of excesses in the 8-9 μm band, showing that it is skewed towards stars displaying positive excesses, with five stars having significance above 3σ. The middle panel shows the same data, but now expressed in zodi units, showing a substantial number of the sample stars having excesses in the range of 150-450 zodis. Note also, the third panel, which includes the entire 8-13 um band also shows a histogram skewed towards positive zodi excess with about 8 stars having excesses above 2σ. (Adapted from Mennesson et al. [30]).

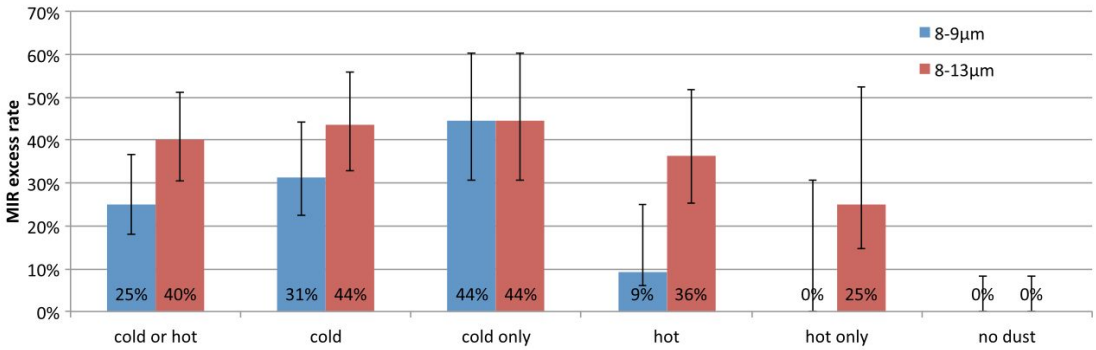

Figure 3. Excess rates observed in the mid-infrared by the Keck Nuller are compared with those known to have either far-infrared (cold), or near-infrared (hot) excesses, or none previously observed. For the Keck Nuller data in the 8-9 μm band, the mid-infrared (MIR) excess rate is defined as requiring and excess with significance greater than 3σ. For the observations from 8 to 13 μm, only a significance of 2σ is used in the figure. Note that there is a strong correlation between detections of a cold excess at far-infrared (FIR) wavelengths, e.g., from Herschel or Spitzer SED observations at 70 μm or longer wavelengths, and the detection of a mid-infrared excess. (Adapted from Mennesson et al. [30]).

3. THE LBTI HOSTS PROGRAM

3.1 The LBTI Instrument and Its Unique Discovery Space for Exozodi Studies

The LBTI has emerged as the best current instrument for improved detection limits for warm debris disks and exozodi studies around nearby stars. The outstanding performance of the LBTI results from a number of unique instrumental features. The LBTI has only three warm reflections before the cold optics of the Universal Beam Combiner (UBC) as well as adaptive secondaries with high-order wavefront correction that provides very high Strehl ratios at N band (>98%). The UBC feeds the components of the LBTI, consisting of NOMIC, the mid-infrared camera and nuller, as well as LMIRCAM, an additional camera operating at L and M bands. The throughput (transmission) to the detector is ~20% and the emissivity is very low, <10%, giving it the highest photometric sensitivity of any ground-based

interferometer operating in the mid-infrared. The expected photometric uncertainty is 0.01% compared to 0.3% for the Keck Interferometer Nuller (KIN).

Besides the high photometric sensitivity, the angular resolution of the LBTI is well-suited to observations of warm debris disks. The first bright fringe is located at an angular distance of $\lambda/(2B)$ from the central dark fringe, where λ is the wavelength of observation and B is the baseline. For the case of LBTI at 10 μm and with a center-to-center spacing of 14.4 m for the two 8.4-m diameter mirrors, the first bright fringe is located at 72 milliarcsec (mas), close to the angular size of 1 AU at 10 pc, which is 100 mas, corresponding to warm dust in the habitable zone at an earth distance from a star like the Sun.

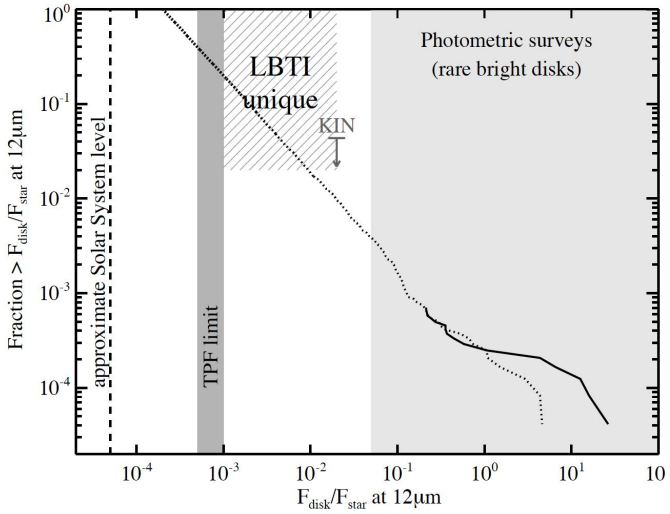

Figure 4. Luminosity function for stars between 0 and 13 Gyr old. The solid line denotes the observed distribution function based on photometric surveys and the dotted line is an extrapolated luminosity function assuming an in situ collisional model consistent with the observational data. The limit from the KIN survey is shown and the unique space occupied by the LBTI survey is shown by the cross-hatched region on the plot. (Kennedy et al. [31]).

The NOMIC camera itself includes the nuller (NIL) at N band and PhaseCam, which operates at H and K bands to stabilize the null within NIL. NOMIC includes a cold field stop with two slits, a pupil wheel with dual and single apertures of varying sizes, dual 12-hole non-redundant aperture masks, and dual spider-annuli masks. The filter wheels include a variety of set of narrow band filters (0.7 μm wide centered at 7.9, 8.9, 9.1, 9.8, 11.9, 12.5 μm), wide filters (N′ -- 9.9-12.4 μm, also 8-13.8 μm, 8.1-9.4 μm, 10.1-11.1 μm), 18 μm and 24 μm filters, and a grism for low-resolution spectroscopy. Further details of the LBTI instrument can be found in the contributions to this conference by Hinz et al. [9] and Defrère et al. [10] mentioned previously.

The importance of LBTI to the study of exozodiacal dust can be seen in Figure 4, which displays an extrapolated luminosity function for exozodiacal dust disks (Kennedy et al. [31]). In this figure the dark line displays the observed luminosity function, which exists only for the dusty stars observed in the photometric surveys discussed previously. An extrapolated luminosity function, assuming an in situ collisional model consistent with the observational data, is shown by the dotted line. The LBTI uniquely explores the luminosity function at the low fractional luminosity levels. Limits for TPF and an upper limit derived from the KIN survey are also displayed in this figure.

4. RECENT PUBLICATIONS FROM THE HOSTS PROGRAM

4.1 Target Selection

A paper describing the target selection methodology and results was published this past year (Weinberger et al. [32]). Figure 5 summarizes the key results of the target selection paper. Two sample types have been determined based on three different methods. For FGK stars, which are of greatest interest for exoplanet direct imaging missions, two differing selection methods were compared, one we call the *Mission Oriented Selection* is determined by applying a target selection code derived from work on the New Worlds Observer (Turnbull et al. [33]), and the other is a *Mission*

Independent Selection derived from the Unbiased Nearby Survey (UNS) sample (Phillips et al. [34]). Both selection methods were applied to stars with spectral types later than F5 and resulted in a sample of 49 nearby sun-like stars, which we call the *"Sun-like Sample"*. A second sample is called the *"Sensitivity Sample"*, and it consists of stars earlier than F4 for which the LBTI has the best sensitivity. This sample consists of 26 stars of spectral type A0-F4, 12 of which have known excesses. This second sample will allow us to probe the exozodi luminosity function at the lowest levels, allowing for a potential extrapolation to the luminosity function of FGK stars in the *Sun-like Sample*, and it also allows us to correlate cold dust from those stars in this sample with known excesses with detections of warm dust from LBTI, which can give us greater insight into the dynamics and evolution of exozodiacal dust. The main exclusions for the two samples were binaries with separation less than 1.5 arcsec and all the stars had to have declination greater than -30 degrees.

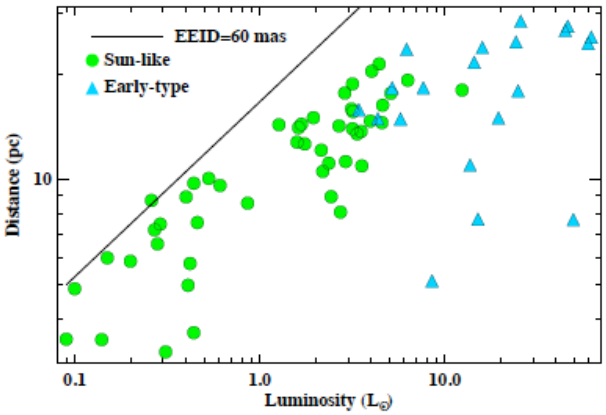

Figure 5. The complete sample for the HOSTS program discussed in Weinberger et al. [32] is shown, with green circles denoting the Sun-like Sample of 48 nearby solar type stars (late F, G, and K spectral types) and the blue triangles denoting the sensitivity driven Early-type Sample of 20 additional (early F and A stars). Note that stars falling below the black line, which denotes the Earth Equivalent Insolation Distance (EEID) of 60 mas. Stars above this line were excluded from the sample because their exozodi emission would be in the first null, making LBTI not very sensitive to this dust. The first transmission peak for LBTI is at 79 mas and the inner working angle is ~39 mas, given the 14.4-m separation of the two primaries (baseline, B) at a wavelength (λ) of 11 μm, and the definition of the inner working angle as λ/(4B), respectively (Adapted fromWeinberger et al. [32]).

4.2 Modeling

Our team created a modeling framework for the LBTI observations in order to determine dust density levels from detections and to place upper limits on the dust levels for non-detections. A paper describing this effort was recently published (Kennedy et al. [35]). LBTI observations of thermal dust emission can be converted into predictions and upper limits for scattered light observations. In this way the LBTI observations will help optimize the target list for individual stars and as a class for visible wavelength direct imaging missions such WFIRST-AFTA, Exo-C, Exo-S, and ATLAST that are currently in a study phase. The modeling effort connects simple physical models of dust disks with the well-known modeling program `zodipic` [36], which utilizes the Kelsall model [6] of our own zodiacal dust. The modeling effort also allows for predictions of the sensitivity of LBTI for the two target samples discussed in the previous section. Figure 6 displays such a prediction assuming the LBTI reaches a stabilized null depth of 10^{-4}, with the *Sun-like* sample shown in the red open circles and the *Sensitivity* sample shown in the blue open squares. Note that the bulk of the stars in the *Sun-like* sample from K0 to F0 have detectable zodi limits from about 10 to 3 zodies, while the *Sensitivity* sample stars are clustered near the Solar System zodi level and even lower for the most luminous stars A stars in the sample. This figure clearly shows that the LBTI has the potential to determine the zodi levels of nearby stars, both individually and as a class, necessary to formulate the direct imaging missions in support of the Astro2010 Decadal Survey goals.

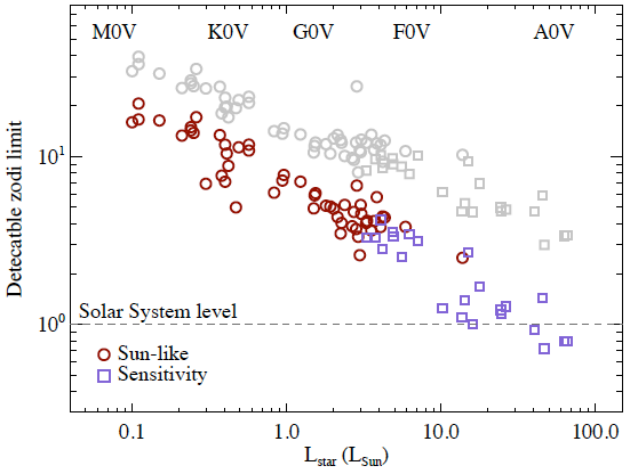

Figure 6. Prediction of LBTI sensitivity limits in terms of solar system zodi units as a function of stellar luminosity assuming the LBTI reaches a stabilized null depth of 10^{-4}. Stars from the *Sun-like* sample are denoted by the red open circles and the *Sensitivity* sample by the blue open squares. The zodi level for the Solar System is indicated by the dashed line. The gray symbols indicate limits for a pessimistic narrow-disk scenario where the disks cover the habitable zone only from 320 to 210K (Kennedy et al. [35]).

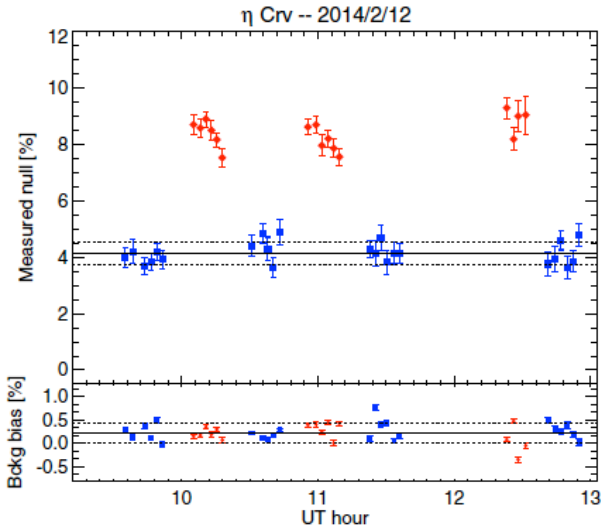

Figure 7. The red symbols denote the measurements of η Crv and the blue symbols are measurements of the calibrator stars for each Observing Block (OB) as a function of Universal Time (UT), as discussed in Defrère et al. [37] The black line is an average of the calibrator measurements, and the average error in the null measurements for the calibrators is indicated by the dotted lines. The estimated instrumental null floor is shown in the lower panel. The excess is detected in the N′ band (9.81-12.41 μm) over a field-of-view of ~140 mas in radius, corresponding to ~2.6 AU at the distance of η Crv (Defrère et al. [37]).

4.3 First science results: η Corvi

Our first science results were obtained during a commissioning run in February 12, 2014, with the star η Crv. A paper describing these results was also published in 2015, in Defrère et al. [37]. Three hours of nulling data were taken near transit. Details of the observations and modeling are presented in the paper. Figure 7 displays null leakage measurements from the LBTI as a function of observation time in UT hours. The red diamond symbols denote the measurements of η Crv and the blue square symbols display measurements of the calibrator stars. The black line is an average of the calibrator measurements. The dotted lines are the average of the error in the null measurements for the calibrators. The estimated instrumental null floor is shown in the lower panel. This is a clear detection of the warm disk around η Crv,

which had previously been detected with the Spitzer IRS instrument with an excess of 17% [38], and an excess of 4% observed with the Keck Interferometer Nuller (Millan-Gabet et al. [27]).

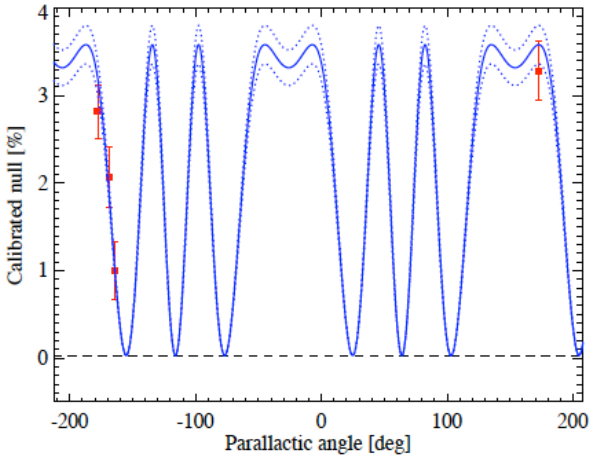

Figure 8. The red squares denote calibrated nulls obtained on the bright G8III+A3IV binary system γ Per (angular separation of 252 mas) on UT December 31, 2013. The solid blue line shows the expected source null using the well-known orbital parameters for this system and the estimated flux ratio in the N' band (see the published paper for more information). The dotted lines correspond to the 1-σ uncertainty on the flux ratio while the black dash line represents the geometric null floor due to the finite extension of the primary. (Adapted from Defrère et al. [39])

4.4 Nulling Data Reduction and On-Sky Performance of LBTI

In a recent paper by Defrère et al. [39], the LBTI team reported progress on the LBTI HOSTS program as of the end of the commissioning phase in the spring of 2015. This paper discussed the theory of operation of the LBTI as a nulling interferometer, data reduction methods, and on sky performance. Substantial progress on wavefront control, phase stabilization, and data reduction methodology allowed LBTI to reach a calibrated null of 0.05% in February 2015 on the A3V star β Leo. This result is equivalent to a measuring an exozodi disk density of 15 to 30 solar system zodis at 10 pc for a Sun-like star, using the adopted disk model discussed previously in the paper by Kennedy et al. [35].

Figure 8 displays an example of the on-sky performance of the nuller observations of the binary system γ Per. The solid blue line shows the expected source null using the well-known orbital parameters for this system and the estimated flux ratio in the N' band (see the published paper for more information). The dotted lines correspond to the 1-σ uncertainty on the flux ratio while the black dash line represents the geometric null floor due to the finite extension of the primary.

The new results from LBTI set a new record for high-contrast interferometric imaging in the near-infrared, and provides a new opportunity for not only studies of debris disks around nearby stars, but substantial additional science of protoplanetary and exoplanetary systems.

5. CURRENT STATUS

The LBTI HOSTS project passed its Operational Readiness Review (ORR) and entered into the Science Verification Phase (SVP) in the Spring of 2015. Figure 9 summarizes the status of the LBTI project at the time of the ORR in terms of its sensitivity defined as the luminosity ration of the dust to the star at a particular dust temperature, e.g., L_{dust}/L_{star}. Note that the LBTI was reaching a level of approximately 12 solar system zodis in three hours of integration, slightly extrapolated from a measurement of 15 zodis in a shorter integration time.

Improvements to the fringe stability are expected as improvements to the phasing camera software control loops are underway including a feed forward system to reduce the effect of telescope vibration. Also, progress has been made on reducing the contribution of fluctuations in the Precipitable Water Vapor (PWV) between the two telescopes to the nulling floor. The SVP was supposed to start in the second semester of 2015 at the LBTI, however, a failure of the Adaptive Secondary system on one of the telescopes precluded the start of the SVP until the Spring of 2016. Spectacularly bad weather over about 1 dozen nights, led to the LBTI operating with the dome open for only about one night in total. Even so, the LBTI team was able to show that the system reached the previous performance level and is

on track to achieve the ultimate expected performance. There is ongoing work at the LBT Observatory to characterize and reduce telescope vibrations, although the low frequency vibrations (less than 20 Hz) are reduced by the feed forward system. See the recent paper by Defrère et al. [10] for a discussion of some of these aspects of the continued performance improvements expected next year.

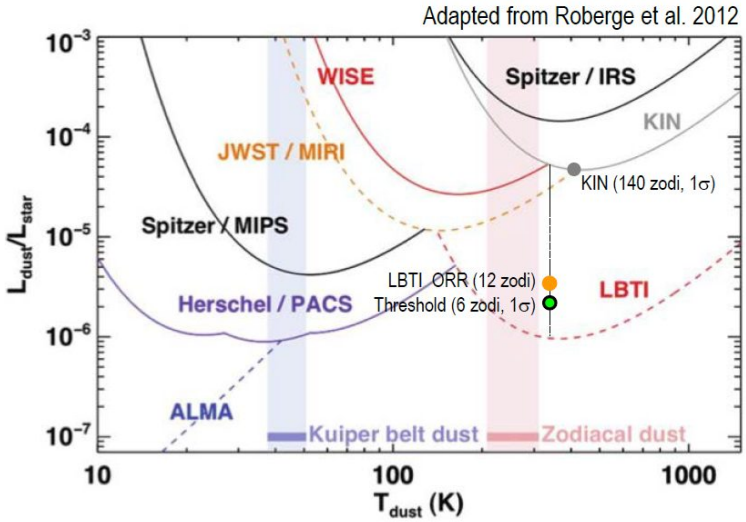

Figure 9. Comparison of the sensitivity of major instruments as a function of dust temperature, using L_{dust}/L_{star} as a measure of sensitivity, where L_{dust} is the luminosity of dust and L_{star} is the luminosity of a star. Note that LBTI has the best sensitivity of all existing and near-term instruments for dust between 150 and 1000 K, including the MIRI instrument on JWST. The performance of the LBTI as of the Operational Readiness Review (ORR) in the Spring of 2015 is shown by the orange circle. The green circle denotes expected performance after additional improvements to the system are made. The ORR value is equivalent to 12 solar system zodi for a Sun-like star at 10 pc. Actual measurement error was 500 ppm (15 zodi) for a Solar-type star at 10 pc. The ORR limit (orange filled circle) of 12 zodi (400 ppm) is based on a small extrapolation of additional observing time, and it is more than 10 times better than that obtained by the Keck Interferometer Nuller several years ago. (Adapted from Roberge et al. [4]).

6. SUMMARY AND CONCLUSIONS

The LBTI HOSTS project will for the first time measure exozodi levels around nearby direct imaging sun-like target stars at the level of 10 times or lower than that of the solar system zodiacal dust level. Two types of target samples have been selected. One is called the "Sun-like" sample and it consists of 48 stars with spectral types later than F5; the other is called the "Sensitivity" sample and it consists of 20 stars having spectral types earlier than F4. For the latter sample, dust levels of the order of one solar system zodi or lower can be expected for some of the stars having the earliest spectral types.

The LBTI HOSTS project passed its Operational Readiness Review (ORR) and entered into the Science Verification Phase (SVP) in the Spring of 2015. Improvements to the fringe stability are expected as improvements to the phasing camera software control loops are underway including a feed forward system to reduce the effect of telescope vibration. Also, progress has been made on reducing the contribution of fluctuations in the Precipitable Water Vapor (PWV) between the two telescopes to the nulling floor.

The first detection of warm zodiacal dust was achieved during commissioning with a clear detection of dust around η Crv. Papers discussing the target selection process and target list, modeling, and first results on η Crv were published in refereed journals in 2015, and a new paper on the technical aspects of LBTI including the nulling data reduction methodology and the on sky performance was published earlier this year. The SVP was supposed to start in the second semester of 2015 at the LB, however, a failure of the Adaptive Secondary mirror on one of the telescopes precluded the start of the SVP until the Spring of 2016. Spectacularly bad weather over about 1 dozen nights, led to the LBTI operating with the dome open for only about one night in total. Even so, the LBTI team was able to show that the system reached the previous performance level and is on track to achieve the ultimate expected performance.

At the next SPIE conference we hope to provide measurements of the luminosity function for the zodiacal dust level around nearby main sequence stars representative of target stars of upcoming and proposed direct imaging missions. Also we plan to explore the correlations between observations of the hot, cold, and warm dust in debris disks in order to further understand the physical processes governing their formation and evolution.

7. ACKNOWLEDGMENTS

The research described in this paper is supported by the Astrophysics Division of the National Aeronautics and Space Administration and the Large Binocular Telescope Observatory, and by a grant from the European Union through ERC grant number 279973 (GMK & MCW).

REFERENCES

[1] Lawson, P. R., Traub, W. A., and Unwin, S. C. (editors), "Exoplanet Community Report," JPL Publication 09-3, Chapters 2 and 4 (2009).
[2] Stapelfeldt, K. et al, Exo-C final report (2015).
[3] Seager, S. et al., Exo-S final report (2015).
[4] Blandford, R. et al., "New Worlds, New Horizons," Astro2010 Decadal Survey, National Academies Press, Washington, DC (2010).
[5] Roberge, A. et al., PASP, 124, 799 (2012).
[6] Kelsall, T. et al., ApJ, 508, 44 (1998).
[7] Defrère, D. et al., Proc. SPIE, Vol. 8442, 84420M, 1 (2012).
[8] Stark, C. & Kuchner, M., ApJ, 707, 543 (2009).
[9] Hinz, P. et al., paper 9907-03, this conference (2016).
[10] Defrère, D. et al., paper 9907-50, this conference, (2016).
[11] Mennesson et al. paper 9907-32, this conference (2016).
[12] Rieke, G. et al., ApJS, 154, 25 (2004).
[13] Rieke, G. et al., ApJ, 620, 1020 (2005).
[14] Bryden, G. et al., ApJ, 705, 1206 (2009).
[15] Lawler, S. et al., ApJ, 705, 89 (2009).
[16] Bryden, G. et al., ApJ, 636, 1098 (2006).
[17] Siercho, J. M. et al., ApJ, 785, 33 (2014).
[18] Eiroa, C. et al., A&A, 555, A11 (2013).
[19] Montesinos, B. et al. A&A in press, arXiv:1605.05837 (2016).
[20] Di Folco, E. et al., A&A, 475, 243 (2007).
[21] Absil, O. et al, A&A, 487, 1041 (2008).
[22] Absil, O. et al. Proc. SPIE, Vol. 88445, 84450X-1, (2012).
[23] Bracewell, R., Nature, 274, 780 (1978).
[24] Barry, R. K. et al., ApJ, 677, 1253 (2008).
[25] Serabyn, E. et al., ApJ, 748, 55 (2012).
[26] Liu, W. et al., ApJ, 693, 1500 (2009).
[27] Millan-Gabet, R. et al., ApJ, 734, 67 (2011).
[28] Colavita, M. et al., PASP, 121, 1120 (2009).
[29] Colavita, M. et al., PASP, 122, 795 (2010).
[30] Mennesson et al., ApJ, 707:119, 1 (2014).
[31] Kennedy, G. & Wyatt, M. MNRAS, 433, 2334 (2013).
[32] Weinberger, A. et al., ApJSS 216:24, 1 (2015).
[33] Turnbull, M. et al., PASP, 124, 418 (2012).
[34] Phillips, N. et al. MNRAS, 403, 1089 (2010).
[35] Kennedy, G. et al., ApJSS, 216:23, 1 (2015).

[36] Kuchner, M., freely available software package.
[37] Defrère, D. et al. ApJ, 799:42, 1 (2015)
[38] Lisse, C. et al., ApJ, 747, 93 (2012).
[39] Defrère, D. et al., ApJ, 824, 66D (2016).